

Electronic Supplementary Information

Ferroelectric, Flexoelectric and Photothermal Coupling in PVDF based Composites for Flexible Photoelectric Sensors

Lu Wang,^a Muzaffar Ahmad Boda,^a Chen Chen,^a Xiang He,^a Zhiguo Yi^{*ab}

^aState Key Laboratory of High Performance Ceramics and Superfine Microstructure, Shanghai Institute of Ceramics, Chinese Academy of Sciences, Shanghai 200050, China. Email:

zhiguo@mail.sic.ac.cn

^bCenter of Materials Science and Optoelectronic Engineering, University of Chinese Academy of Sciences, Beijing 100049, China

This PDF file includes:

Experimental section

Figs. S1 to S8

Table S1

Other Supplementary Materials for this manuscript include the following:

Video S1

Experimental Section

Ceramic particles preparation: Firstly, raw materials BaCO₃ (99.0%), BaZrO₃ (99.0%), CaCO₃ (99.0%), TiO₂ (98.0%) and MnO₂ (99%) are mixed and pre-sintered at 1300 °C for 4 h by traditional solid phase sintering method, then the mixture is ball-milled for 12 h to obtain the 0.5Ba(Zr_{0.08}Ti_{0.8}Mn_{0.12})O₃-0.5(Ba_{0.7}Ca_{0.3})TiO₃ (BZTM-BCT) powders. Next, 0.2 g BZTM-BCT particles are dispersed into 10 ml deionized water, followed by the addition of 4 ml 80 mmol/L sodium citrate solution and 4ml 20 mmol/L H₂AuCl₄ solution. After stirring at 100 °C for 30 min, the mixture is cleaned by deionized water and ethanol for some times, and dried at 60 °C for 2 h to obtain the BZTM-BCT:Ag particles. Likewise, BZTM-BCT:Ag particles are prepared by magnetically stirring 0.2 g BZTM-BCT and 0.2 g AgNO₃ powders in 12 ml ethylene glycol at 100 °C for 2 h, followed by cleaning and drying procedures as carrying out in case of BZTM-BCT:Ag particles.

PVDF composite film preparation: Different ceramic particles including BZT-BCT, BZTM-BCT, Au-BZTM-BCT and Ag-BZTM-BCT particles with the mass of 0.1 g are dispersed into 10 g N,N-Dimethylformamide (DMF) while stirring for 1 h to avoid their agglomeration. Subsequently, 1 g PVDF powders are added into these suspensions and then kept for stirring at 40 °C for 6 h to make the PVDF fully dissolved. To obtain a dense PVDF composite films, the precursor solutions are coated on the polyethylene terephthalate (PET) film by a simple tape casting method and vacuum dried at 45 °C for 4 h, followed by annealing at 120 °C for 2 h to improve the crystallinity. The obtained films are named as PVDF, PVDF/BZT-BCT, PVDF/BZTM-BCT, PVDF/BZTM-BCT:Ag and PVDF/BZTM-BCT:Ag, respectively.

Characterization: The crystal structure of the ceramic particles and the films are studied by an X-Ray diffractometer (XRD, Bruker D8 ADVANCE, Germany) with Cu K_α radiation. Microstructures of the films were characterized by a desktop scanning electron microscopy (SEM, Phenom Pro, Holland). The appearances and selected area electron diffraction (SAED) of the Au and Ag loaded BZTM-BCT particles are characterized by high resolution transmission electron microscopy (HRTEM, JEOL JEM-F200, Japan). Film phase structures were analyzed by using Fourier Transform Infrared Spectrometer (FTIR, Thermo Fisher Scientific Nicolet iS50R, USA). Valance states of elements were studied by X-Ray photoelectron spectroscopy (XPS, Thermo Scientific K_α). The photo absorbance and transmission are collected by a PerkinElmer Lambda 900 UV-Vis-NIR spectrometer, in which BaSO₄ is covered on

the integrating sphere as a reference. Temperature measurement is conducted by a thermocouple. For photoelectric measurements, the samples were cut to the size of $2 \times 2 \text{ cm}^2$. The Ag and ITO electrodes were coated and deposited on the two sides with area of 2.89 cm^2 , respectively. Before testing, the samples were DC poled at 50 MV/m for 30 min and then the photovoltaic properties were tested by a Keithley 6517B. The used light sources are LED light with different wavelengths.

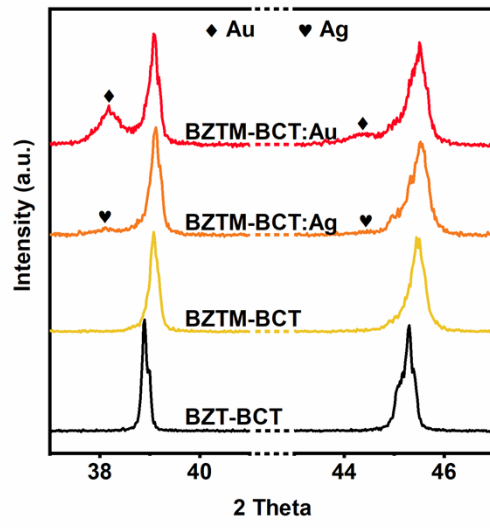


Fig. S1 The extracted and enlarged part in the XRD spectra from 37° to 41° and from 43° to 47°.

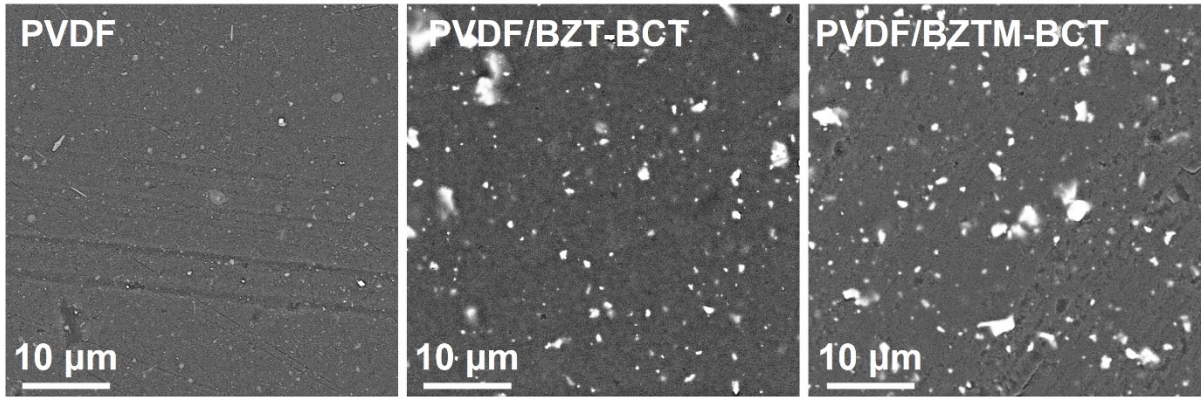


Fig. S2 The surface topography of Pure PVDF, PVDF/BZT-BCT and PVDF/BZTM-BCT films.

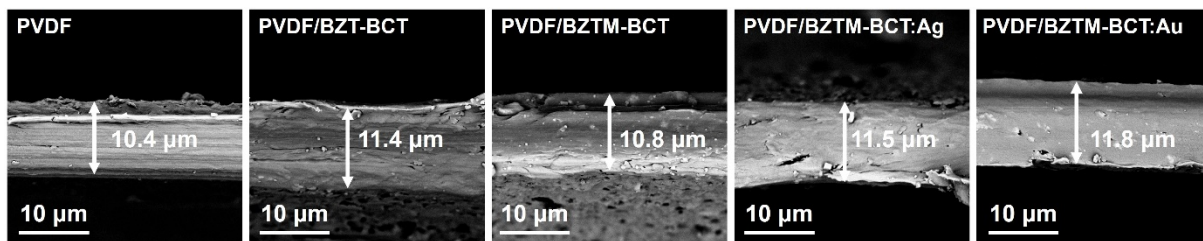


Fig. S3 The cross-section of the five different composite films.

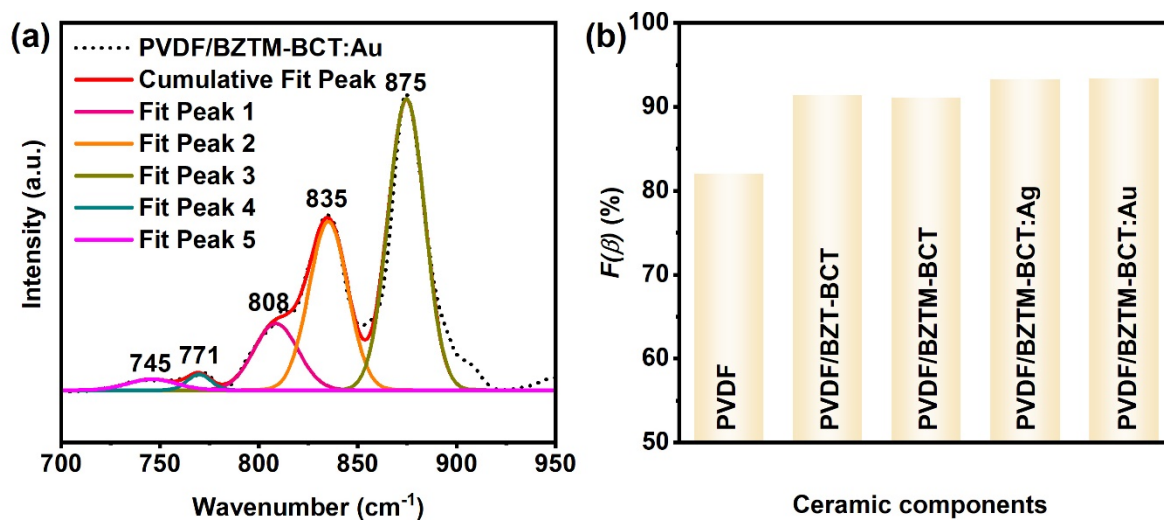


Fig. S4 FTIR analysis of PVDF composite films. (a) Fitting curves of the FTIR curve of PVDF/BZTM-BCT:Au from 700 to 950 cm⁻¹. (b) The β phase contents of different PVDF composite films.

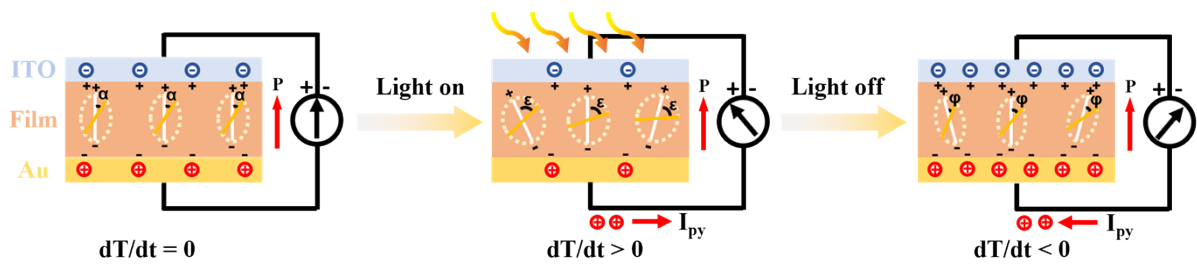


Fig. S5 Schematical diagram of pyroelectric mechanism.

Fig. S5 schematically explains the pyroelectric mechanism of the poled film. When the film is in dark condition, the polarized dipoles are at stable stage and no generation of pyroelectric current. When light turns on, increasing film temperature disturbs random oscillation state of dipoles, resulting in larger oscillation angle, so the average polarization is decreased. As a result, the bound charges on the film surface are reduced, accompanied by current flowing from ITO to Au electrodes. Pyroelectric current is dependent on temperature change rate dT/dt . Because film temperature rising rate gradually decreases, the pyroelectric current exhibits a peak current at the moment when light turns on, and then gradually decreases to about zero under constant light illumination. When light turns off, opposite polarization change induces opposite pyroelectric peak current

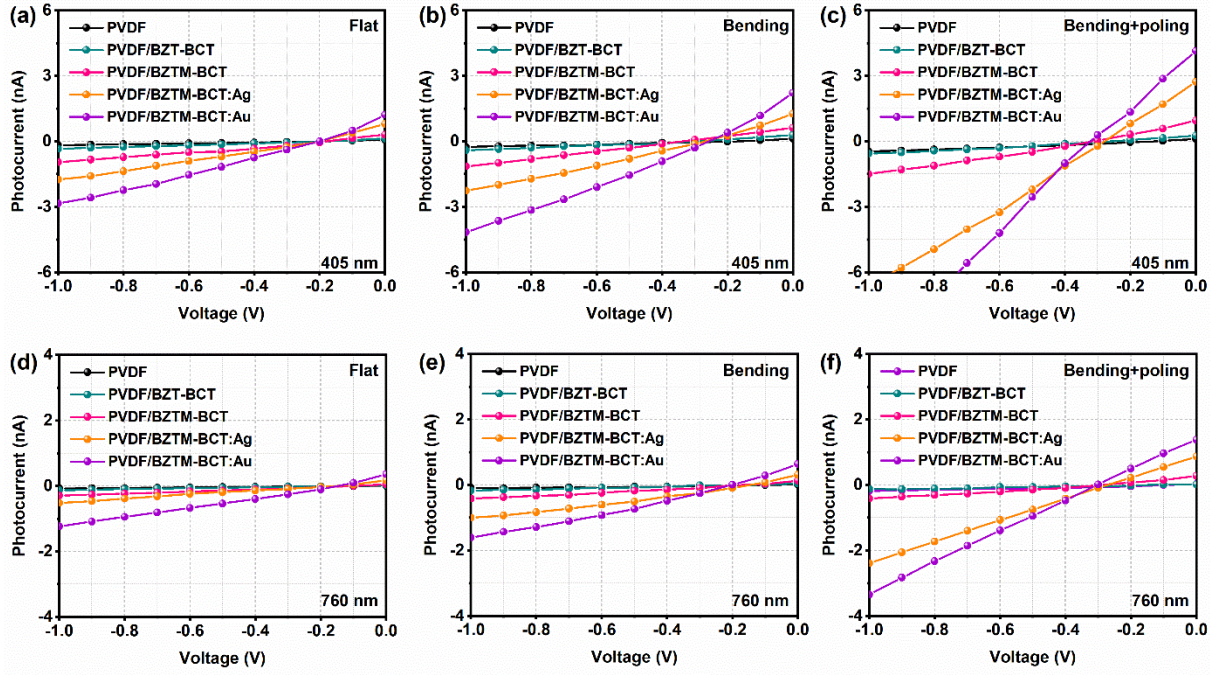


Fig. S6 Photocurrent-time curves of five films under three stages irradiated by 405 nm (a-c) and 760 nm (d-f) light of 100 mW/cm².

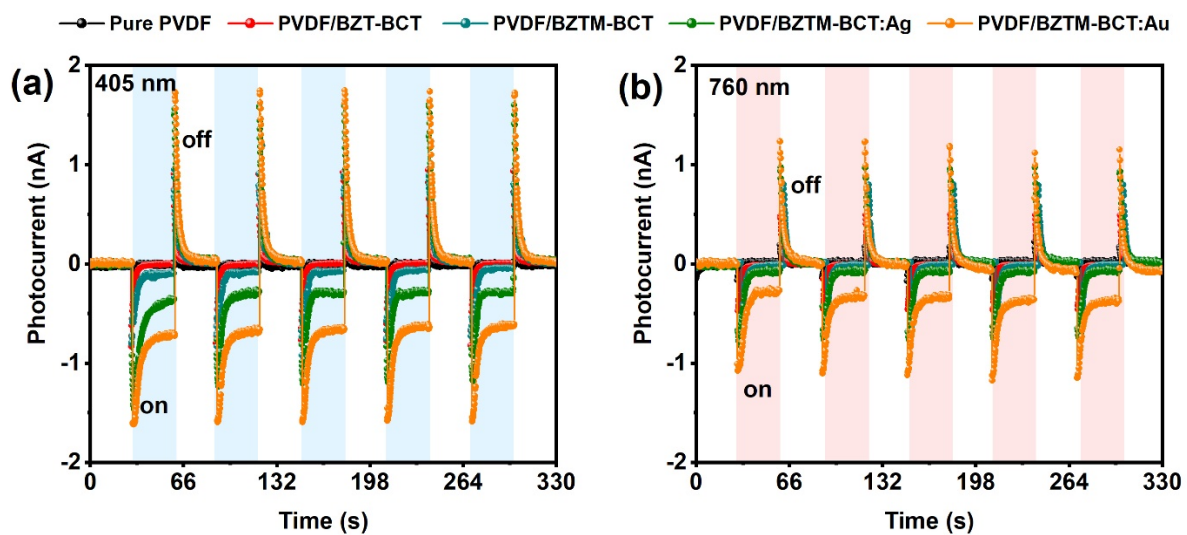


Fig. S7 Photocurrent-time curves of upward samples under downward poling under 405 nm and 760 nm light illumination.

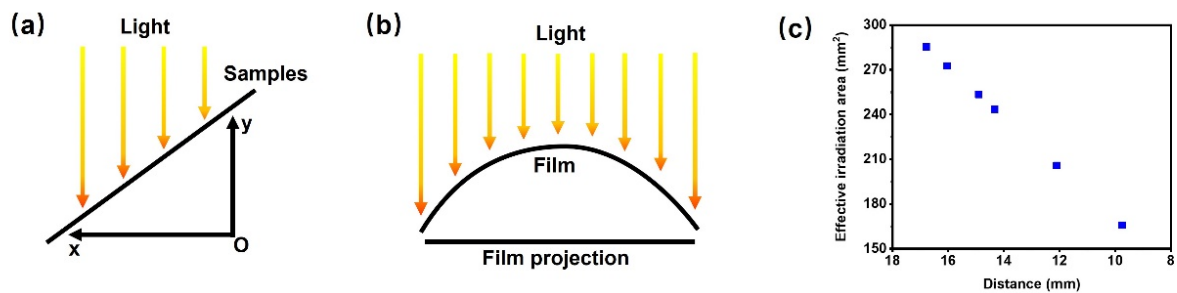


Fig. S8 Calculation of effective irradiation area of the bending film under light illumination. As shown in Fig. S8 a and b, when the bending film is irradiated by uniform light, only the projection on x axis can be effectively irradiated, while the projection on the y axis cannot. The projection area on x axis of the bending film is present in Fig. S8c.

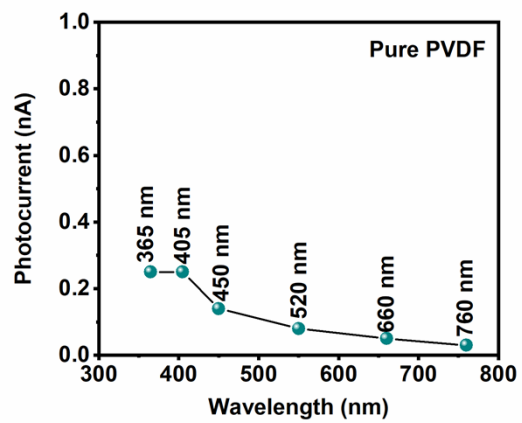


Fig. S9 Photocurrent dependence on photo wavelength, with light intensity of 100 mW/cm².

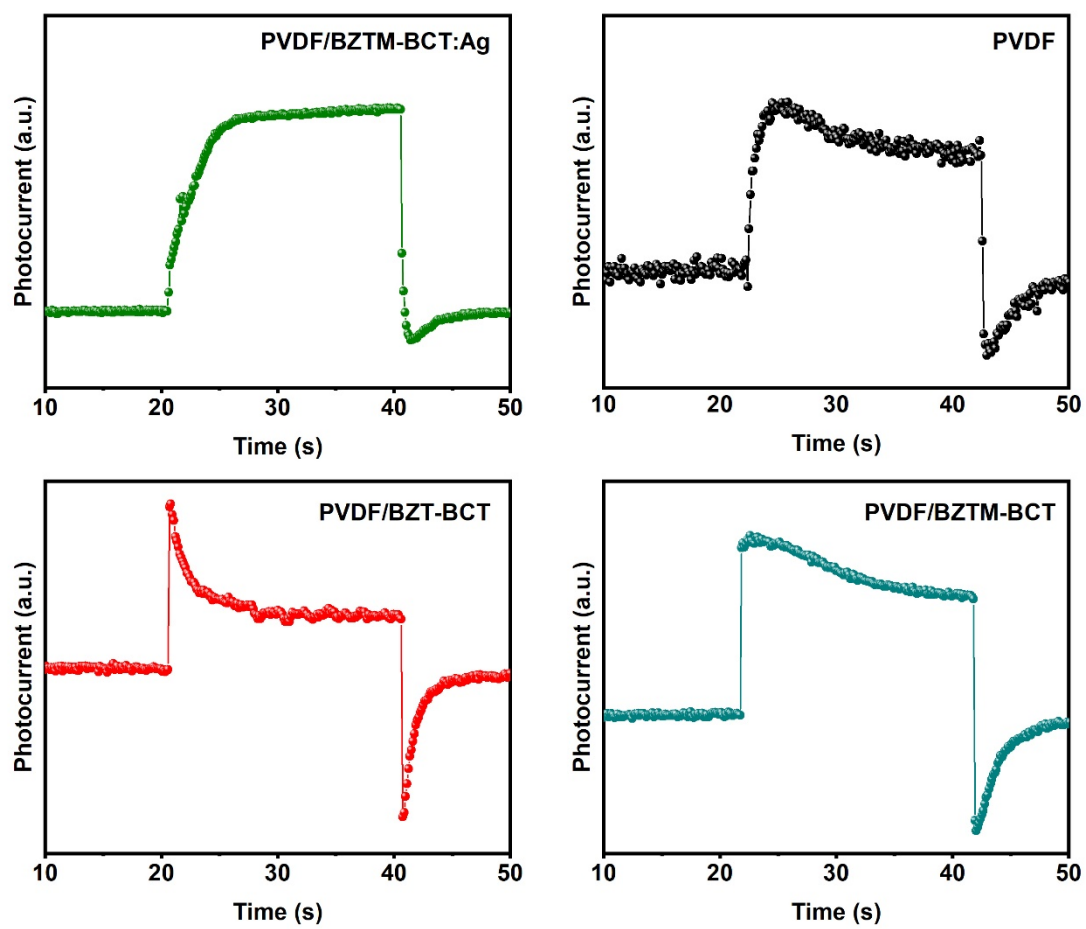


Fig. S10 Photocurrent-time curves of other films under laser 405 nm at 100 mW/cm².

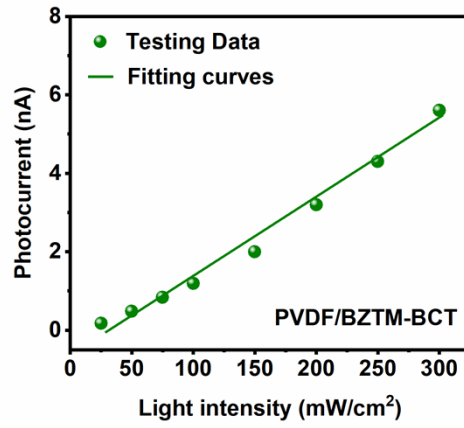


Fig. S11 Photocurrent-light intensity curves of PVDF/BZTM-BCT composite film.

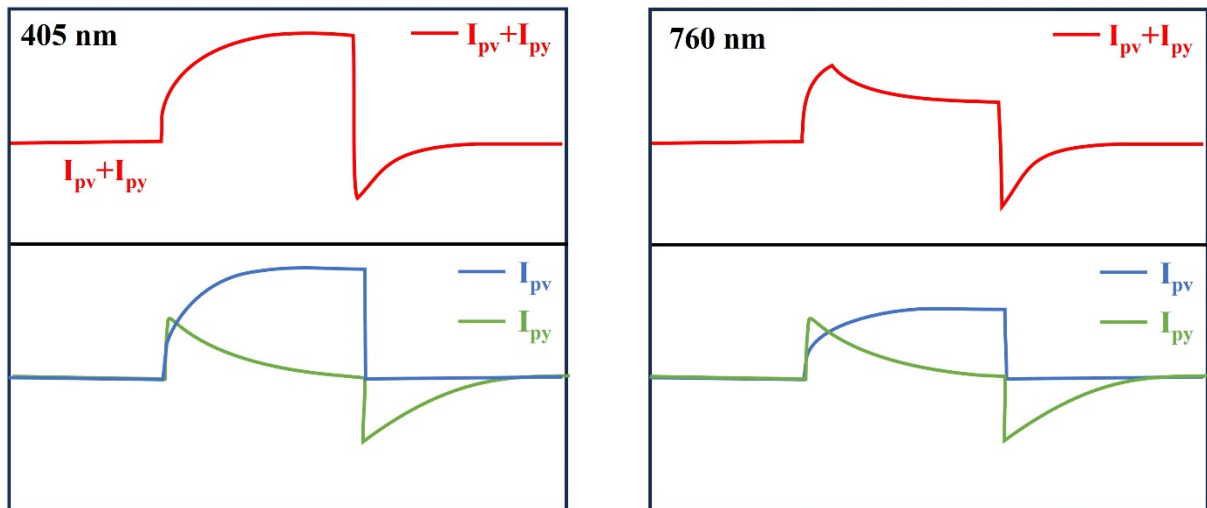


Fig. S12 Photocurrent composition of PVDF/BZTM-BCT:Ag and PVDF/BZTM-BCT:Ag composite films.

Table S1. Comparison of the photocurrent of the five composites under three different states.

Samples	Photocurrent under different states (nA)				
	I_{Flat}	I_{Bending}	$I_{\text{Bending}} - I_{\text{Flat}}$	$I_{\text{Bending + poling}}$	$I_{\text{Bending + poling}} - I_{\text{Bending}}$
PVDF	0.07	0.16	0.09	0.24	0.08
PVDF/BZT-BCT	0.12	0.34	0.22	0.38	0.04
PVDF/BZTM-BCT	~0.28	0.73	0.45	~0.96	0.23
PVDF/BZTM-BCT:Ag	0.79	1.31	0.52	2.75	1.44
PVDF/BZTM-BCT:Au	1.21	2.16	0.95	~4.02	1.86